sodium deoxycholate, 0.1% sodium dodecyl sulfate and 1× protein inhibitor cocktail (Nacalai tesque, Kyoto, Japan), phosphate-buffered saline; pH 7.4). After incubation on ice for 15 minutes, the lysate was centrifuged at 10,000*g* for 15 minutes at 4°C. The protein content of the supernatants was determined using a bicinchoninic acid protein assay kit (Pierce, Rockford, IL). Equal amounts of protein were electrophoretically separated by sodium dodecyl sulfate polyacrylamide gels (8% or 12%) and transferred onto polyvinylidene fluoride membrane. For immunodetection, the following antibodies were used: anti–Bcl-xL antibody (Santa Cruz Biotechnology, Santa Cruz, CA), anti–Mcl-1 antibody (Rockland, Gilbertsville, PA), anti-Bax antibody (Cell Signaling Technology, Beverly, MA), anti-Bid antibody (Cell Signaling Technology), anti-albumin antibody (Affinity Bioreagents, Golden, CO), and anti–beta actin antibody (Sigma-Aldrich, Saint Louis, MO). Detection of immunolabeled proteins was performed using a chemiluminescent substrate (Pierce).

Neonate Analysis. Neonatal mice delivered by cesarean section were suckled by a surrogate mother and sacrificed at 10 hours after birth. Blood from the neonatal mice was centrifuged, and the plasma was stored at −20°C until use. The levels of total bilirubin and ammonia were measured by Van den Bergh reaction and a standard enzymatic procedure, respectively, at Oriental Kobo Life Science Laboratory.

Real-Time Reverse-Transcription PCR. Total RNA was prepared from liver tissue using RNeasy kit (QIAGEN, Tokyo, Japan). For complementary DNA synthesis, 1 μg total RNA was reverse-transcribed using the High Capacity RNA-to-DNA Master Mix (Applied Biosystems, Foster City, CA). Complementary DNA, equivalent to 40 ng RNA, was used as a template for real-time reverse-transcription PCR (RT-PCR) using an Applied Biosystems 7900HT Fast Real-Time PCR System (Applied Biosystems). The messenger RNA expressions of tumor necrosis factor alpha (TNF-α), collagen-alpha1(I), and transthyretin were measured using TaqMan Gene Expression Assays (Assay ID: Mm00443260_g1, Mm00801666_g1, and Mm00443267_m1, respectively), and were corrected with the quantified expression level of beta-actin messenger RNA measured using TaqMan Gene Expression Assays (Assay ID: Mm02619580_g1).

Statistical Analysis. Data are presented as mean ± standard deviation. Comparisons between two groups were performed by unpaired *t* test. Multiple comparisons were performed by analysis of variance followed by Scheffe *post hoc* correction. $P < 0.05$ was considered statistically significant.

Results

Hepatocyte-Specific Mcl-1 Deficiency Leads to Spontaneous Hepatocyte Apoptosis in the Adult Liver. To generate hepatocyte-specific Mcl-1–deficient mice, floxed *mcl-1* mice were crossed with heterozygous *AlbCre* mice. After *mcl-1*$^{flox/+}$ *AlbCre* mice were mated with *mcl-1*$^{flox/+}$ mice, and offspring were screened for genotyping and Mcl-1 expression. *mcl-1*$^{flox/flox}$ *AlbCre* mice were born and grew up. Their expression in the liver of Mcl-1 was greatly reduced compared with that of wild-type mice (Fig. 1A). The levels of Bcl-xL expression did not change in *mcl-1*$^{flox/flox}$ *AlbCre* liver. Bcl-xL and Mcl-1 proteins migrated as typical doublet bands of which the biochemical nature had been previously determined.[18] The trace amount of Mcl-1 expression found in the knockout liver may have been attributable to expression in nonparenchymal cells, as previously observed in hepatocyte-specific Bcl-xL–deficient mice.[13]

To investigate the significance of Mcl-1 in the liver, mice were sacrificed 6 weeks after birth and subjected to analysis of serum ALT levels and caspase-3/7 activity as well as liver histology and TUNEL staining. *mcl-1*$^{flox/flox}$ *AlbCre* mice displayed significantly higher levels of serum ALT than control mice (*AlbCre*-negative or *mcl-1*$^{+/+}$ *AlbCre* mice) (Fig. 1B). Hepatocytes with typical apoptosis morphology such as cellular shrinkage and nuclear condensation were frequently observed in the liver sections of *mcl-1*$^{flox/flox}$ *AlbCre* mice (Fig. 1C). Consistently, the number of cells with TUNEL positivity, a hallmark of apoptotic cell death, in the liver was significantly higher in *mcl-1*$^{flox/flox}$ *AlbCre* mice than in control mice (Fig. 1C). Activity of caspase-3/7, executioners of apoptosis, was significantly higher in circulation of *mcl-1*$^{flox/flox}$ *AlbCre* mice than in control mice, which might reflect activation of those proteases in the knockout liver (Fig. 1D). Bax expression was clearly increased in *mcl-1*$^{flox/flox}$ *AlbCre* mice, suggesting Bax activation being involved in the apoptosis in *mcl-1*$^{flox/flox}$ *AlbCre* mice (Fig. 1A). Furthermore, the expression of TNF-α and collagen-alpha1(I) was significantly increased in the *mcl-1*$^{flox/flox}$ *AlbCre* liver compared with the wild-type liver, as found in the Bcl-xL knockout liver (Fig. 1E). Taken together, hepatocyte-specific Mcl-1 knockout mice developed spontaneous apoptosis leading to sterile inflammation and fibrotic response in the liver, like hepatocyte-specific Bcl-xL knockout mice.[13]

Heterozygous Deletion of the mcl-1 Gene Does Not Produce Apoptosis But Increases the Susceptibility to Fas Stimulation. Although the levels of Mcl-1 expression were significantly decreased in *mcl-1*$^{flox/+}$ *AlbCre* liver (Fig. 1A, Supporting Fig. 1), *mcl-1*$^{flox/+}$ *AlbCre* mice did not have apoptosis phenotypes in the liver (Fig. 1B-D).

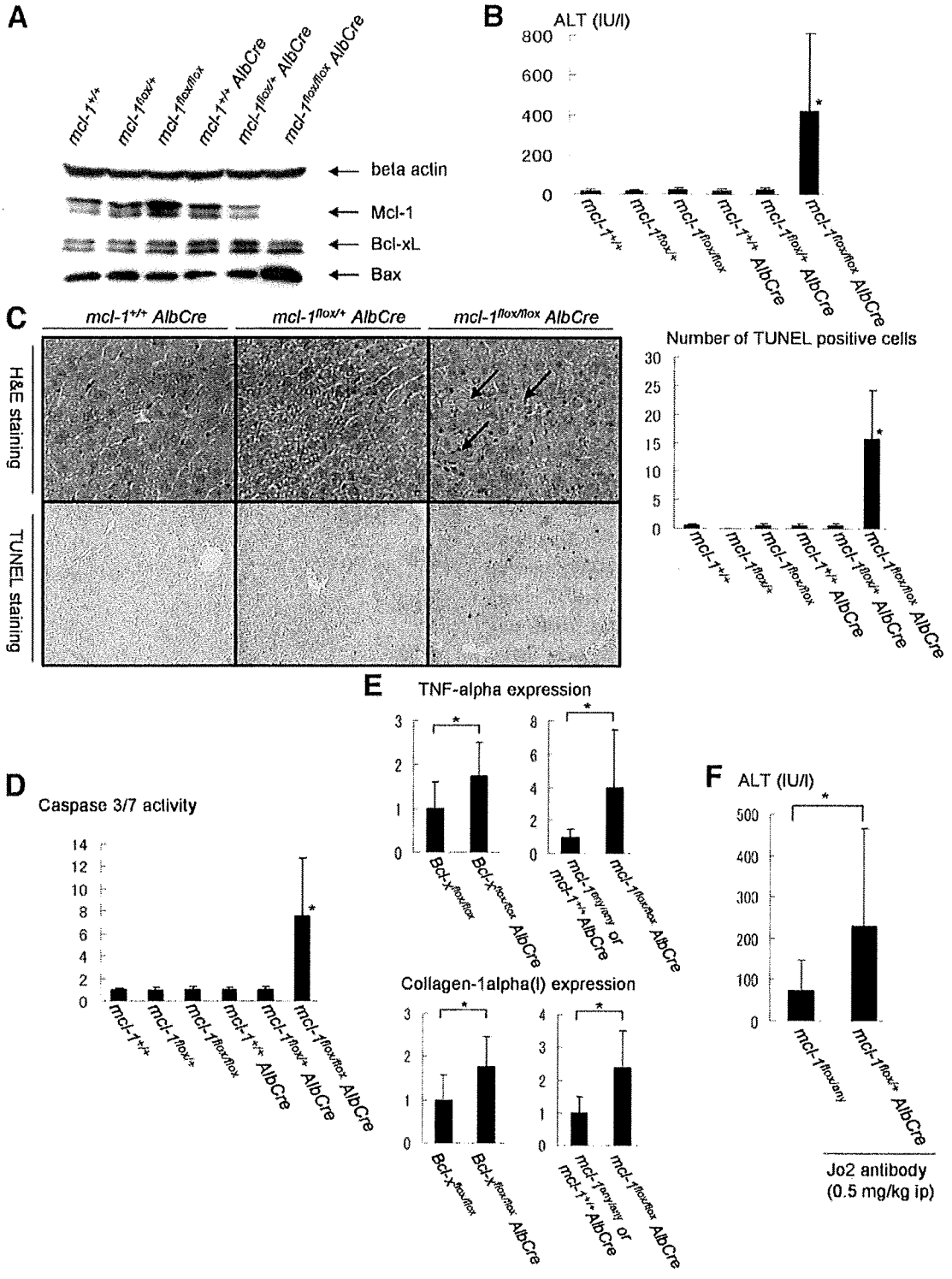

Fig. 1. Hepatocyte-specific Mcl-1 knockout mice. Offspring from mating of *mcl-1*$^{flox/+}$ *AlbCre* mice and *mcl-1*$^{flox/+}$ mice were sacrificed at the age of 6 weeks. (A) Western blot of whole liver lysate for the expression of Bcl-xL, Mcl-1, and Bax. (B) Serum ALT levels. N = 15 mice for each group. *$P < 0.05$ versus the other five groups. (C) Left panel shows hematoxylin-eosin and TUNEL staining of the liver section. Arrow indicates typical apoptotic cells. Right panel shows statistics of TUNEL-positive cells. The number of TUNEL-positive cells was determined in a defined area. N = 5 mice for each group. *$P < 0.05$ versus the other five groups. (D) Serum levels of caspase-3/7 activity. The levels were normalized to *mcl-1*$^{+/+}$ *AlbCre* (−) mice. N = 15 mice for each group. *P < 0.05 versus the other five groups. (E) Real-time RT-PCR analysis for TNF-α and collagen-1alpha(1) expression. *$P < 0.05$. N = 12 or 9. The levels were normalized to the wild-type mice. (F) Serum ALT levels of Fas-stimulated mice. The *mcl-1*$^{flox/+}$ *AlbCre* mice and *mcl-1*$^{flox/+ \text{ or } flox}$ mice were sacrificed 3 hours after intraperitoneal injection of 0.5 mg/kg Jo2 antibody. *$P < 0.05$. N = 13 or 7.

Therefore, we examined the susceptibility to Fas stimulation in these mice. We injected anti-Fas antibody into *mcl-1*$^{flox/+}$ *AlbCre* mice and *mcl-1*$^{flox/+\ or\ flox}$ mice and measured the levels of their serum ALT. *mcl-1*$^{flox/+}$ *AlbCre* mice displayed significantly higher levels of serum ALT than control mice (Fig. 1F). These findings suggest that haplo-deficiency of Mcl-1 does not produce apoptosis in a physiological setting but clearly reduces apoptosis resistance under pathological conditions.

Involvement of Bid in Apoptosis Caused by Mcl-1 Deficiency. BH3-only proteins regulate life and death balance by interacting with core Bcl-2 family members. The hepatocyte is a so-called type 2 cell, which requires Bid as a sensor for Fas-mediated apoptotic stresses.[19] In addition, it has been reported that the caspase-8/Bid pathway is involved in a variety of liver pathological conditions.[16,20] To examine the possibility of Bid being involved in hepatocyte apoptosis caused by Mcl-1 deficiency, we crossed hepatocyte-specific Mcl-1 knockout mice with Bid knockout mice. Offspring form mating of *bid*$^{+/-}$ *mcl-1*$^{flox/flox}$ *AlbCre* mice with *bid*$^{+/-}$ *mcl-1*$^{flox/flox}$ mice were sacrificed at 6 weeks after birth and subjected to analysis of apoptosis phenotypes. Mice with each genotype grew up, and, as expected, the levels of Bid and/or Mcl-1 expression in the liver were correspondingly reduced with their genotypes (Fig. 2A). The levels of serum ALT were significantly lower in *bid*$^{-/-}$ *mcl-1*$^{flox/flox}$ *AlbCre* mice than in *bid*$^{+/+}$ *mcl-1*$^{flox/flox}$ *AlbCre* mice (Fig. 2B). The results indicate that Bid was involved in hepatocyte apoptosis found in Mcl-1 knockout mice.

Combined Deficiency of Mcl-1 and Bcl-xL in Hepatocytes Causes Lethality. Phenotypes observed in hepatocyte-specific Mcl-1 knockout mice were very similar to those in hepatocyte-specific Bcl-xL knockout mice.[13] These results indicated that Bcl-xL and Mcl-1 share similar anti-apoptotic functions but do not compensate for the loss of each other. To examine whether their expression and function are completely nonredundant or just partially so, we generated hepatocyte-specific Bcl-xL/Mcl-1 double-knockout mice.

The *bcl-x*$^{flox/+}$ *mcl-1*$^{flox/+}$ *AlbCre* mice were mated with *bcl-x*$^{flox/flox}$ *mcl-1*$^{flox/flox}$ mice, and genotypes of the offspring were screened at 3 weeks after birth. *AlbCre*-negative and *bcl-x*$^{flox/+}$ *mcl-1*$^{flox/+}$ *AlbCre* mice were born and grew up, but not *bcl-x*$^{flox/flox}$ *mcl-1*$^{flox/+}$ *AlbCre*, *bcl-x*$^{flox/+}$ *mcl-1*$^{flox/flox}$ *AlbCre*, and *bcl-x*$^{flox/flox}$ *mcl-1*$^{flox/flox}$ *AlbCre* mice (Table 1). The lack of Bcl-xL and Mcl-1 caused a more severe phenotype than either knockout, suggesting that they partially compensate for the loss of each other at least from the viewpoint of maintaining normal development.

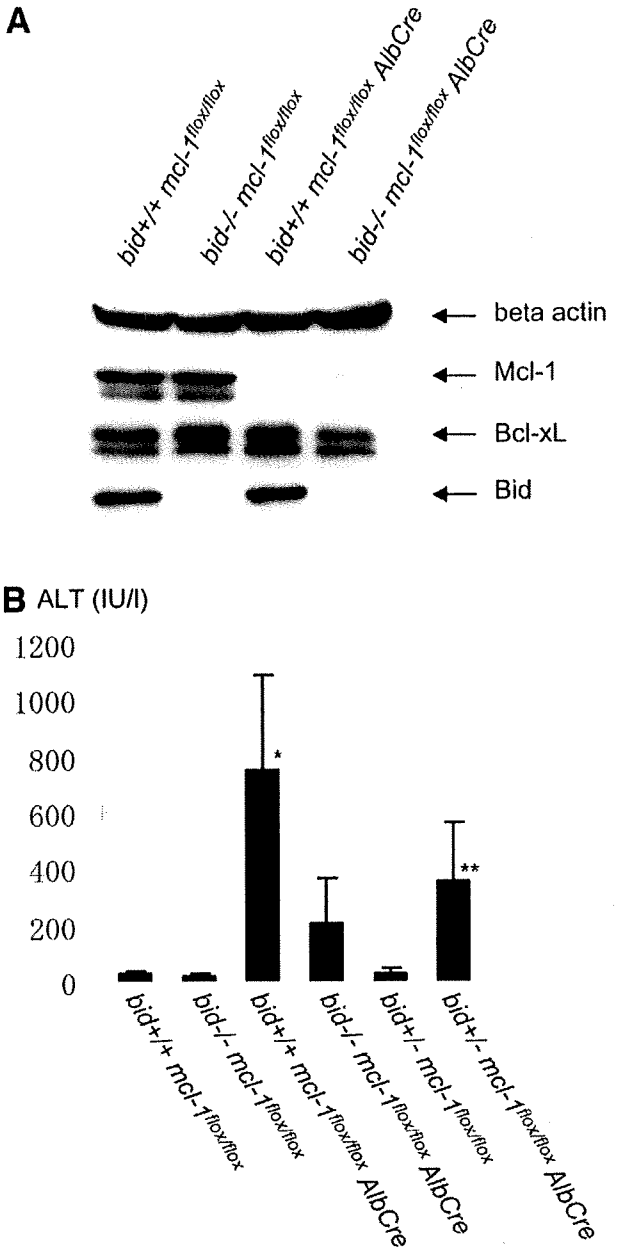

Fig. 2. Mcl-1/Bid double-knockout mice. Offspring from mating of *bid*$^{+/-}$ *mcl-1*$^{flox/flox}$ *AlbCre* mice with *bid*$^{+/-}$ *mcl-1*$^{flox/flox}$ mice were sacrificed at 6 weeks after birth. (A) Western blot of whole liver lysate for the expression of Mcl-1, Bcl-xL, and Bid. (B) Serum ALT levels. N = 12 mice for each group. *$P < 0.05$ versus the other five groups; **$P < 0.05$ versus the *AlbCre*-negative groups and the *bid*$^{+/+}$ *mcl-1*$^{flox/flox}$ *AlbCre* group.

Mice Lacking Single Alleles for Both Bcl-xL and Mcl-1 Develop Spontaneous Apoptosis in the Adult Liver Similar to Bcl-xL or Mcl-1 Knockout Mice. Offspring from mating of *bcl-x*$^{flox/+}$ *mcl-1*$^{flox/+}$ *AlbCre and bcl-x*$^{flox/flox}$ *mcl-1*$^{flox/flox}$ were sacrificed at 6 weeks after birth and subjected to analysis of Bcl-xL/Mcl-1 expression and

Table 1. Genotyping of Offspring Obtained by Crossing *bcl-x*$^{flox/+}$ *mcl-1*$^{flox/+}$ *AlbCre* Mice and *bcl-x*$^{flox/flox}$ *mcl-1*$^{flox/flox}$ Mice

AlbCre	bcl-x	mcl-1	ED18.5	3 Weeks
−	flox/+	flox/+	4	14
−	flox/flox	flox/+	6	17
−	flox/+	flox/flox	12	17
−	flox/flox	flox/flox	7	17
+	flox/+	flox/+	11	22
+	flox/flox	flox/+	8	0
+	flox/+	flox/flox	9	0
+	flox/flox	flox/flox	10	0
	Total		67	87

ED, embryonic day.
Note that each genotype is expected to account for one-eighth of the offspring from this mating.

apoptosis phenotypes. As expected, *bcl-x*$^{flox/+}$ *mcl-1*$^{flox/+}$ *AlbCre* liver expressed reduced levels of expression for both Bcl-xL and Mcl-1 (Fig. 3A). Interestingly, *bcl-x*$^{flox/+}$ *mcl-1*$^{flox/+}$ *AlbCre* mice developed spontaneous hepatocyte apoptosis as evidenced by an increase in serum ALT levels and caspase-3/7 activity (Fig. 3B,C). In agreement with this, hepatocytes with typical apoptotic morphology and positive for TUNEL staining were found scattered in the liver lobules in these mice (Fig. 3D,E). Furthermore, *bcl-x*$^{flox/+}$ *mcl-1*$^{flox/+}$ *AlbCre* mice showed higher expression of TNF-α than wild-type mice (Fig. 3F). The phenotypes were very similar to hepatocyte-specific Bcl-xL or Mcl-1knockout mice.

Hepatocyte-Specific Mcl-1/Bcl-xL-Deficient Mice Show Impaired Development of the Liver and Liver Failure During the Neonatal Period. To examine the impact of Bcl-xL/Mcl-1deficiency at an earlier time point, offspring obtained from crossing *bcl-x*$^{flox/+}$ *mcl-1*$^{flox/+}$ *AlbCre* mice and *bcl-x*$^{flox/flox}$ *mcl-1*$^{flox/flox}$ mice were analyzed on gestational day 18.5. Live-obtained embryo followed expected Mendelian frequencies (Table 1). Overall, they looked normal, and their body weight did not differ among genotypes (Fig. 4A,B). However, the livers obtained from live pups with genotype of *bcl-x*$^{flox/flox}$ *mcl-1*$^{flox/+}$ *AlbCre*, *bcl-x*$^{flox/+}$ *mcl-1*$^{flox/flox}$ *AlbCre*, or *bcl-x*$^{flox/flox}$ *mcl-1*$^{flox/flox}$ *AlbCre* were clearly smaller. The ratios of liver weight to body weight were significantly lower in those pups than in *AlbCre*-negative or *bcl-x*$^{flox/+}$ *mcl-1*$^{flox/+}$ *AlbCre* pups (Fig. 4C). The ratios of liver weight to body weight were also examined in *mcl-1*$^{flox/flox}$ with *AlbCre* or without *AlbCre* mice, and there was no significant difference between the two (6.0 ± 0.8 versus 5.5 ± 0.9, N = 5, $P = 0.34$), excluding the possibility that Mcl-1 knockout itself affects the liver size at this time point. Histological analysis revealed that there were a number of hepatocytes with rectangular morphology and hematopoietic cells in the developing liver of the *AlbCre*-negative pups (Fig. 4D). Whereas the number of rectangular hepatocytes in *bcl-x*$^{flox/+}$ *mcl-1*$^{flox/+}$ *AlbCre* livers was similar to that in the *AlbCre*-negative livers, it was lower in *bcl-x*$^{flox/flox}$ *mcl-1*$^{flox/+}$ *AlbCre*, *bcl-x*$^{flox/+}$ *mcl-1*$^{flox/flox}$ *AlbCre*, and *bcl-x*$^{flox/flox}$ *mcl-1*$^{flox/flox}$ *AlbCre* livers. Rectangular cells were rarely observed in *bcl-x*$^{flox/flox}$ *mcl-1*$^{flox/flox}$ *AlbCre* livers. Furthermore, the expression of albumin and transthyretin was examined in the liver as a marker for hepatocyte differentiation.[21] Consistent with histological findings, both expressions were gradually reduced from the *AlbCre*-negative livers to the *bcl-x*$^{flox/flox}$ *mcl-1*$^{flox/flox}$ *AlbCre* livers (Fig. 4E,F).

We noticed that offspring obtained from crossing *bcl-x*$^{flox/+}$ *mcl-1*$^{flox/+}$ *AlbCre* mice and *bcl-x*$^{flox/flox}$ *mcl-1*$^{flox/flox}$ mice frequently died within 1 day after birth. To examine the cause of the early neonatal death, offspring were sacrificed at 10 hours after birth. They were divided into two groups according to the data shown in Table 1: expected survivors including *AlbCre*-negative and *bcl-x*$^{flox/+}$ *mcl-1*$^{flox/+}$ *AlbCre* pups, and expected nonsurvivors including *bcl-x*$^{flox/flox}$ *mcl-1*$^{flox/+}$ *AlbCre*, *bcl-x*$^{flox/+}$ *mcl-1*$^{flox/flox}$ *AlbCre*, and *bcl-x*$^{flox/flox}$ *mcl-1*$^{flox/flox}$ *AlbCre* pups. The levels of total bilirubin and ammonia in circulation were determined and compared between the groups. Both blood bilirubin levels and ammonia levels were significantly higher in the expected nonsurvivors than in the expected survivors (Fig. 5A,B). These results suggested that *bcl-x*$^{flox/flox}$ *mcl-1*$^{flox/+}$ *AlbCre*, *bcl-x*$^{flox/+}$ *mcl-1*$^{flox/flox}$ *AlbCre*, and *bcl-x*$^{flox/flox}$ *mcl-1*$^{flox/flox}$ *AlbCre* mice died quickly after birth because of hepatic failure, in agreement with the findings of impaired liver development.

Discussion

Five members of the anti-apoptotic Bcl-2 family have been found: Bcl-2, Bcl-xL, Bcl-w, Bfl-1, and Mcl-1. Traditional knockout of Bcl-2, a prototype of this family, displays growth retardation, hair color abnormality, lymphocyte decrease, and polycystic kidney.[22,23] In agreement with the finding that Bcl-2 is not expressed in hepatocytes,[13] these mice did not show any liver phenotypes. Similarly, Bcl-w[24,25] or Bfl-1 knockout mice[26] were generated but no liver phenotypes have been reported. Traditional knockout of Bcl-xL or Mcl-1 caused more severe phenotypes. Deletion of the *bcl-x* gene resulted in embryonic lethality because of abnormal neuronal development and hematopoiesis.[27] The *mcl-1* knockout embryo fails to be implanted *in utero*.[28] Thus, study of traditional knockout mice could not reveal the significance of Bcl-xL or Mcl-1 in the liver.

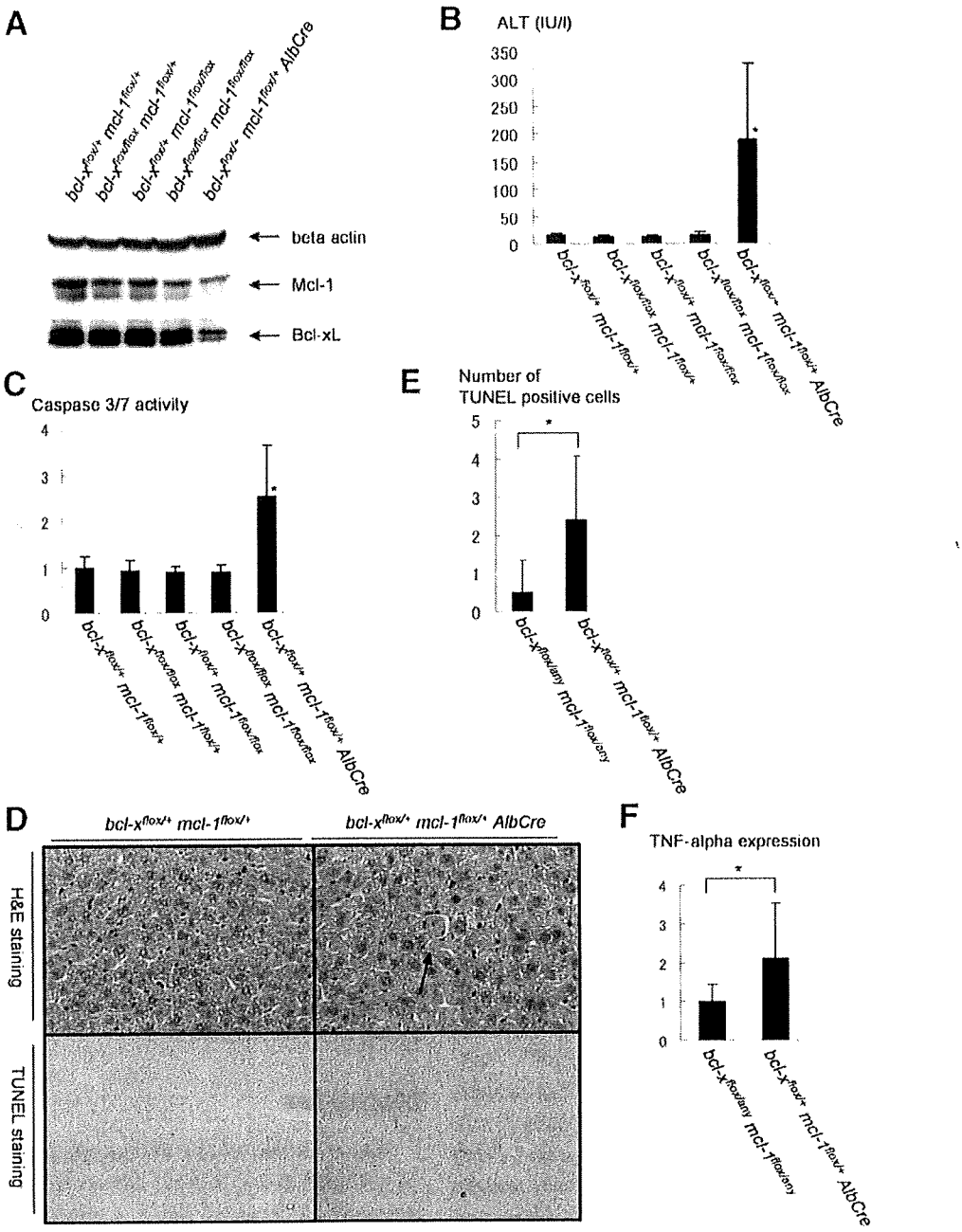

Fig. 3. Hepatocyte-specific Bcl-xL/Mcl-1-deficient mice. Offspring from mating *bcl-x*$^{flox/+}$ *mcl-1*$^{flox/+}$ *AlbCre* mice and *bcl-x*$^{flox/flox}$ *mcl-1*$^{flox/flox}$ mice were sacrificed at the age of 6 weeks. (A) Western blot of whole liver lysate for the expression of Bcl-xL and Mcl-1. (B) Serum ALT levels. N = 9 mice for each group. *$P < 0.05$ versus the other five groups. (C) Serum levels of caspase-3/7 activity. The levels were normalized to *bcl-x*$^{flox/+}$ *mcl-1*$^{flox/+}$ mice. N = 9 mice for each group. *$P < 0.05$ versus the other five groups. (D) Hematoxylin-eosin and TUNEL staining of the liver sections for *bcl-x*$^{flox/+}$ *mcl-1*$^{flox/+}$ *AlbCre* mice. Findings for *bcl-x*$^{flox/+}$ *mcl-1*$^{flox/+}$ mice are shown as a control. (E) Statistics of TUNEL-positive cells. The number of TUNEL-positive cells was determined in a defined area. N = 5 or 6. *$P < 0.05$. (F) RT-PCR analysis for TNF-α expression. The levels were normalized to the group of *bcl-x*$^{flox/+ \text{ or } flox}$ *mcl-1*$^{flox/+ \text{ or } flox}$. *$P < 0.05$. N = 9.

We previously reported that hepatocyte-specific knockout of Bcl-xL caused spontaneous apoptosis in hepatocytes after birth and established that Bcl-xL is critically important for the integrity of hepatocytes.[13] The current study demonstrated that Mcl-1 plays an anti-apoptotic role in differentiated hepatocytes similar to that of Bcl-xL. During the preparation of this manuscript, a report by Vick et al.[29] appeared on the Web, demonstrating a similar apoptosis phenotype in mice with specific knockout of the *mcl-1* gene in hepatocytes. Our findings

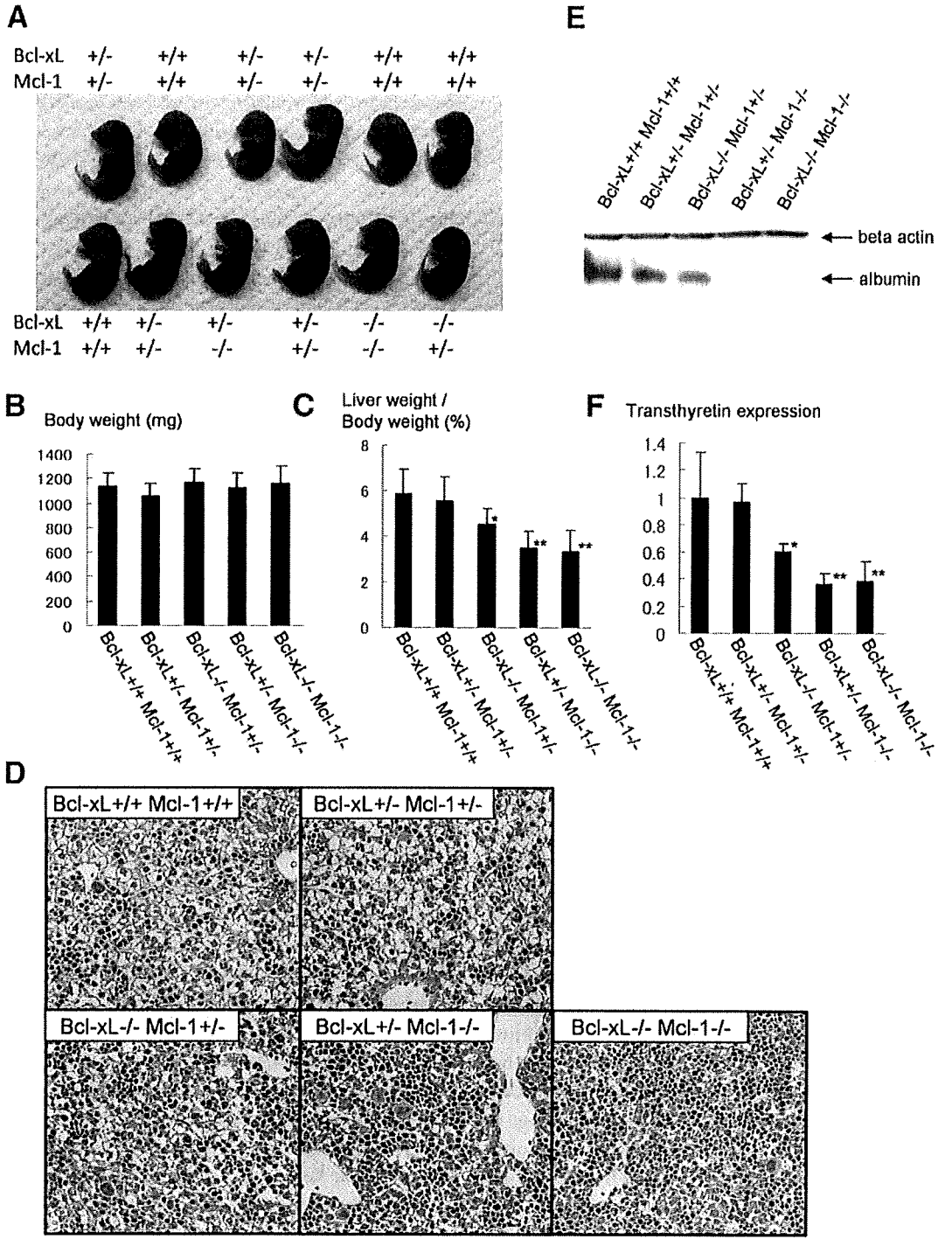

Fig. 4. Hepatocyte-specific Bcl-xL/Mcl-1-deficient embryos. Offspring from mating *bcl-x*$^{flox/+}$ *mcl-1*$^{flox/+}$ *AlbCre* mice and *bcl-x*$^{flox/flox}$ *mcl-1*$^{flox/flox}$ mice were sacrificed on day 18.5 of gestation. Mice were classified into five groups. The *bcl-x*$^{flox/+ \text{ or } flox}$ *mcl-1*$^{flox/+ \text{ or } flox}$ are indicated by Bcl-xL +/+ Mcl-1 +/+; *bcl-x*$^{flox/+}$ *mcl-1*$^{flox/+}$ *AlbCre* are indicated by Bcl-xL +/− Mcl-1 +/−; *bcl-x*$^{flox/flox}$ *mcl-1*$^{flox/+}$ *AlbCre* are indicated by Bcl-xL −/− Mcl-1 +/−; *bcl-x*$^{flox/+}$ *mcl-1*$^{flox/flox}$ *AlbCre* are indicated by Bcl-xL +/− Mcl-1 −/−; *bcl-x*$^{flox/flox}$ *mcl-1*$^{flox/flox}$ *AlbCre* are indicated by Bcl-xL −/− Mcl-1 −/ −. The numbers of embryos analyzed were 30 for Bcl-xL +/+ Mcl-1 +/+, 11 for Bcl-xL +/− Mcl-1 +/−, 8 for Bcl-xL −/− Mcl-1 +/−, 9 for Bcl-xL +/− Mcl-1 −/−, and 10 for Bcl-xL −/− Mcl-1 −/−. (A) Gross appearance of embryos. Representative photo for a litter is shown. (B) Body weight. (C) The ratios of liver weight to body weight. *$P < 0.05$ versus Bcl-xL +/+ Mcl-1 +/+; **$P < 0.05$ versus Bcl-xL +/+ Mcl-1 +/+ and Bcl-xL +/− Mcl-1 +/−. (D) Hematoxylin-eosin staining of the liver sections. (E) Western blot of whole-liver lysate for albumin expression. (F) Real-time RT-PCR analysis for transthyretin expression. The levels were normalized to the group of Bcl-xL +/+ Mcl-1 +/+. *$P < 0.05$ versus Bcl-xL +/+ Mcl-1 +/+; **$P < 0.05$ versus Bcl-xL +/+ Mcl-1 +/+ and Bcl-xL +/− Mcl-1 +/−.

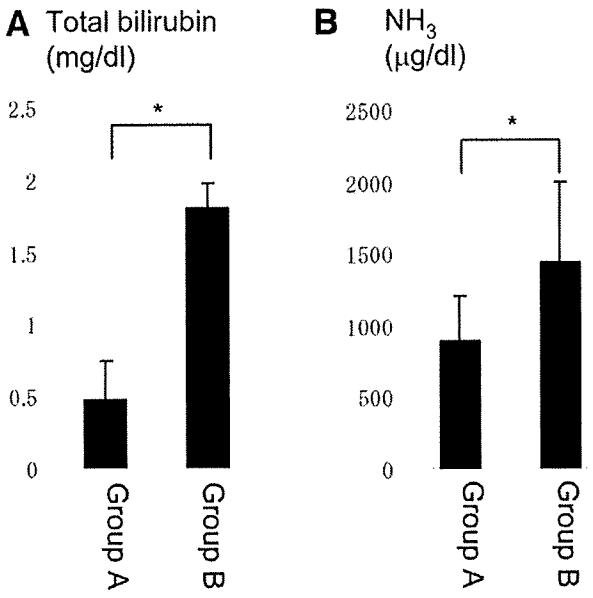

Fig. 5. Plasma biochemistry of hepatocyte-specific Bcl-xL/Mcl-1-deficient neonates 10 hours after birth. Group A (N = 13) was defined as expected survivors including *AlbCre*-negative mice and *bcl-x*$^{flox/+}$ *mcl-1*$^{flox/+}$ *AlbCre* mice. Group B (N = 6) was defined as expected nonsurvivors including *bcl-x*$^{flox/flox}$ *mcl-1*$^{flox/+}$ *AlbCre*, *bcl-x*$^{flox/+}$ *mcl-1*$^{flox/flox}$ *AlbCre*, *bcl-x*$^{flox/flox}$ *mcl-1*$^{flox/flox}$ *AlbCre*. (A) Plasma total bilirubin levels. *$P < 0.05$. (B) Plasma ammonia levels in both groups. *$P < 0.05$.

are in agreement with theirs and further provide evidence that deletion of a single allele for the *mcl-1* gene fails to produce apoptosis phenotypes under physiological conditions, as observed in knockout of the *bcl-x* gene.[13] Mcl-1 heterozygous disrupted mice did not produce apoptosis at least until 16 weeks of age (our unpublished data). It was demonstrated that hepatocyte-specific Mcl-1 knockout mice showed higher levels of liver injury than control mice on anti-Fas antibody injection.[29] However, because mice lacking both *mcl-1* alleles possess preexisting liver injury, it would be difficult to exactly compare liver injury after anti-Fas antibody injection and to conclude whether decreased Mcl-1 expression actually increases the susceptibility to Fas. In the current study, we took advantage of Mcl-1 heterozygous disrupted mice to address this point. They showed significantly higher levels of liver injury after Fas stimulation than wild-type mice, formally proving the significance of Mcl-1 expression under pathological conditions. Furthermore, our data on Mcl-1/Bid–deficient mice implies that the Bid pathway is involved in generating apoptosis found in Mcl-1 knockout mice. Because Bid mediates a variety of cellular stresses in hepatocytes upstream of Mcl-1,[30,31] it will be interesting in future study to determine what stresses generate hepatocyte apoptosis in Mcl-1 knockout mice.

Bcl-xL and Mcl-1 share similar structures and functions.[1] The observations that either deficiency similarly leads to spontaneous hepatocyte apoptosis imply that they play a non-redundant role in maintaining the integrity of hepatocytes in the adult liver. To further understand the relationship of both molecules, we generated hepatocyte-specific Bcl-xL/Mcl-1 knockout mice. Interestingly, mice lacking single alleles for both genes (*bcl-x*$^{+/-}$ *mcl-1*$^{+/-}$) induced spontaneous hepatocyte apoptosis that could not be distinguished from that found in Bcl-xL or Mcl-1 knockout mice. This indicates that, whereas knockout of a single allele of the *bcl-x* or *mcl-1* gene did not produce apoptosis, knockout of two alleles of any combination among both genes was sufficient to produce hepatocyte apoptosis. This finding suggests that both molecules are not independently but rather interdependently required for ensuring integrity of differentiated hepatocytes.

Bcl-xL/Mcl-1-deficient mice as well as mice only having a single allele of either *bcl-x* or *mcl-1* gene displayed a decreased number of hepatocytes and reduced liver size on day 18.5 of gestation and appeared to develop lethal liver failure within 1 day after birth. Because the liver contains a large number of hematopoietic cells during development (Fig. 4D), it is very difficult to determine the expression levels of Bcl-xL or Mcl-1 specifically in hepatocytes in each knockout mouse. Liver development begins on day 8.5 of gestation in the mouse when the liver primordium is delineated from the endoderm.[32] The albumin promoter, which is active in both hepatoblasts and hepatocytes, shows a 20-fold increase in transcriptional activity from day 9.5 to day 12.5 of gestation. The level of albumin then continues to increase as the liver develops simultaneously with the biliary tree and the hepatic bile duct being formed.[33] Thus, the target genes could probably be successfully deleted during embryogenesis in the *AlbCre* recombination system. The observation that Bcl-xL/Mcl-1–deficient mice developed severer phenotypes than Bcl-xL–deficient or Mcl-1–deficient mice supports the idea that Cre-mediated deletion of the target genes actually took place during embryogenesis in our model. In contrast to the knockout of two alleles, knockout of three alleles and more of the *bcl-x* and *mcl-1* genes induced lethal neonatal hepatic failure. Thus, hepatocyte integrity appeared to be strictly controlled by Bcl-xL and Mcl-1 in a gene dose–dependent manner.

Hepatocyte-specific deficiency of both Bcl-xL and Mcl-1 led to significant reduction of liver volume because of impaired hepatocyte development. However, overall, mice with these phenotypes were capable of developing normally until birth and rapidly developed liver failure and died within 1 day after birth. This finding suggests that differentiated hepatocytes are critically required for maintaining host homeostasis after birth but not during embryogenesis. The placenta

plays an important role in nutritional support and detoxification of the embryo. Our data imply that it could probably compensate for most functions of the liver cells during embryogenesis, whereas the liver would turn to the critical organ that is essential for maintaining host homeostasis after birth. Bcl-xL/Mcl-1 knockout mice provide interesting implications for the difference in the impact of differentiated hepatocytes between embryogenesis and the early neonatal period.

In conclusion, Mcl-1 and Bcl-xL are two major Bcl-2 family proteins inhibiting hepatocyte apoptosis. Together with previous work on traditional knockout mice, our data imply that other members, if any, could not compensate for their functions. Mcl-1 and Bcl-xL cooperatively maintain hepatocyte integrity during liver development and in adult liver homeostasis, and their effects are gene-dose dependent. Recent studies also have established that Mcl-1[5-7] and Bcl-xL[18,34] are frequently overexpressed and confer resistance to apoptosis in hepatocellular carcinoma. Therefore, Mcl-1 and Bcl-xL are important apoptosis antagonists in a variety of pathophysiological conditions of the liver.

Acknowledgment: We thank Dr. You-Wen He (Department of Immunology, Duke University Medical Center, Durham, NC) for providing the *mcl-1* floxed mice.

References

1. Youle RJ, Strasser A. The BCL-2 protein family: opposing activities that mediate cell death. Nat Rev Mol Cell Biol 2008;9:47-59.
2. Tsujimoto Y. Cell death regulation by the Bcl-2 protein family in the mitochondria. J Cell Physiol 2003;195:158-167.
3. Fischer U, Jänicke RU, Schulze-Osthoff K. Many cuts to ruin: a comprehensive update of caspase substrates. Cell Death Differ 2003;10:76-100.
4. Wei MC, Zong WX, Cheng EH, Lindsten T, Panoutsakopoulou V, Ross AJ, et al. Proapoptotic BAX and BAK: a requisite gateway to mitochondrial dysfunction and death. Science 2001;292:727-730.
5. Sieghart W, Losert D, Strommer S, Cejka D, Schmid K, Rasoul-Rockenschaub S, et al. Mcl-1 overexpression in hepatocellular carcinoma: a potential target for antisense therapy. J Hepatol 2006;44:151-157.
6. Fleischer B, Schulze-Bergkamen H, Schuchmann M, Weber A, Biesterfeld S, Müller M, et al. Mcl-1 is an anti-apoptotic factor for human hepatocellular carcinoma. Int J Oncol 2006;28:25-32.
7. Schulze-Bergkamen H, Fleischer B, Schuchmann M, Weber A, Weinmann A, Krammer PH, et al. Suppression of Mcl-1 via RNA interference sensitizes human hepatocellular carcinoma cells towards apoptosis induction. BMC Cancer 2006;6:232.
8. Llovet JM, Bruix J. Molecular targeted therapies in hepatocellular carcinoma. HEPATOLOGY 2008;48:1312-1327.
9. Liu L, Cao Y, Chen C, Zhang X, McNabola A, Wilkie D, et al. Sorafenib blocks the RAF/MEK/ERK pathway, inhibits tumor angiogenesis, and induces tumor cell apoptosis in hepatocellular carcinoma model PLC/PRF/5. Cancer Res 2006;66:11851-11858.
10. Casado M, Mollá B, Roy R, Fernández-Martínez A, Cucarella C, Mayoral R, et al. Protection against Fas-induced liver apoptosis in transgenic mice expressing cyclooxygenase 2 in hepatocytes. HEPATOLOGY 2007;45:631-638.
11. Schulze-Bergkamen H, Brenner D, Krueger A, Suess D, Fas SC, Frey CR, et al. Hepatocyte growth factor induces Mcl-1 in primary human hepatocytes and inhibits CD95-mediated apoptosis via Akt. HEPATOLOGY 2004;39:645-654.
12. Baskin-Bey ES, Huang W, Ishimura N, Isomoto H, Bronk SF, Braley K, et al. Constitutive androstane receptor (CAR) ligand, TCPOBOP, attenuates Fas-induced murine liver injury by altering Bcl-2 proteins. HEPATOLOGY 2006;44:252-262.
13. Takehara T, Tatsumi T, Suzuki T, Rucker EB III, Hennighausen L, Jinushi M, et al. Hepatocyte-specific disruption of Bcl-xL leads to continuous hepatocyte apoptosis and liver fibrotic responses. Gastroenterology 2004;127:1189-1197.
14. Dzhagalov I, St John A, He YW. The antiapoptotic protein Mcl-1 is essential for the survival of neutrophils but not macrophages. Blood 2007;109:1620-1626.
15. Wagner KU, Claudio E, Rucker EB 3rd, Riedlinger G, Broussard C, Schwartzberg PL, et al. Conditional deletion of the Bcl-x gene from erythroid cells results in hemolytic anemia and profound splenomegaly. Development 2000;127:4949-4958.
16. Yin XM, Wang K, Gross A, Zhao Y, Zinkel S, Klocke B, et al. Bid-deficient mice are resistant to Fas-induced hepatocellular apoptosis. Nature 1999;400:886-891.
17. Takehara T, Hayashi N, Tatsumi T, Kanto T, Mita E, Sasaki Y, et al. Interleukin 1β protects mice from Fas-mediated hepatocyte apoptosis and death. Gastroenterology 1999;117:661-668.
18. Takehara T, Takahashi H. Suppression of Bcl-xL deamidation in human hepatocellular carcinomas. Cancer Res 2003;63:3054-3057.
19. Scaffidi C, Fulda S, Srinivasan A, Friesen C, Li F, Tomaselli KJ, et al. Two CD95 (APO-1/Fas) signaling pathways. EMBO J 1998;17:1675-1687.
20. Faubion WA, Guicciardi ME, Miyoshi H, Bronk SF, Roberts PJ, Svingen PA, et al. Toxic bile salts induce rodent hepatocyte apoptosis via direct activation of Fas. J Clin Invest 1999;103:137-145.
21. Tosh D, Shen CN, Slack JM. Differentiated properties of hepatocytes induced from pancreatic cells. HEPATOLOGY 2002;36:534-543.
22. Veis DJ, Sorenson CM, Shutter JR, Korsmeyer SJ. Bcl-2-deficient mice demonstrate fulminant lymphoid apoptosis, polycystic kidneys, and hypopigmented hair. Cell 1993;75:229-240.
23. Nakayama K, Nakayama K, Negishi I, Kuida K, Sawa H, Loh DY. Targeted disruption of Bcl-2 alpha beta in mice: occurrence of gray hair, polycystic kidney disease, and lymphocytopenia. Proc Natl Acad Sci U S A 1994;91:3700-3704.
24. Print CG, Loveland KL, Gibson L, Meehan T, Stylianou A, Wreford N, et al. Apoptosis regulator bcl-w is essential for spermatogenesis but appears otherwise redundant. Proc Natl Acad Sci U S A 1998;95:12424-12431.
25. Ross AJ, Waymire KG, Moss JE, Parlow AF, Skinner MK, Russell LD, et al. Testicular degeneration in Bclw-deficient mice. Nat Genet 1998;18:251-256.
26. Hamasaki A, Sendo F, Nakayama K, Ishida N, Negishi I, Nakayama K, et al. Accelerated neutrophil apoptosis in mice lacking A1-a, a subtype of the bcl-2-related A1 gene. J Exp Med 1998;188:1985-1992.
27. Motoyama N, Wang F, Roth KA, Sawa H, Nakayama K, Nakayama K, et al. Massive cell death of immature hematopoietic cells and neurons in Bcl-x-deficient mice. Science 1995;267:1506-1510.
28. Rinkenberger JL, Horning S, Klocke B, Roth K, Korsmeyer SJ. Mcl-1 deficiency results in peri-implantation embryonic lethality. Genes Dev 2000;14:23-27.
29. Vick B, Weber A, Urbanik T, Maass T, Teufel A, Krammer PH, et al. Knockout of myeloid cell leukemia-1 induces liver damage and increases apoptosis susceptibility of murine hepatocytes. HEPATOLOGY 2009;49:627-636.
30. Yin XM. Bid, a BH3-only multi-functional molecule, is at the cross road of life and death. Gene 2006;369:7-19.
31. Malhi H, Gores GJ. Cellular and molecular mechanisms of liver injury. Gastroenterology 2008;134:1641-1654.
32. Kaestner KH. The making of the liver: developmental competence in foregut endoderm and induction of the hepatogenic program. Cell Cycle 2005;4:146-1148.
33. Cascio S, Zaret KS. Hepatocyte differentiation initiates during endodermal-mesenchymal interactions prior to liver formation. Development 1991;113:217-225.
34. Takehara T, Liu X, Fujimoto J, Friedman SL, Takahashi H. Expression and role of Bcl-xL in human hepatocellular carcinomas. HEPATOLOGY 2001;34:55-61.

Hepatology Research 2009; 39: 724–738 doi: 10.1111/j.1872-034X.2009.00509.x

Original Article

Adiponectin prevents progression of steatohepatitis in mice by regulating oxidative stress and Kupffer cell phenotype polarization

Juichi Fukushima,[1] Yoshihiro Kamada,[1] Hitoshi Matsumoto,[1] Yuichi Yoshida,[1] Hisao Ezaki,[1] Takayo Takemura,[1] Yukiko Saji,[1] Takumi Igura,[1] Shusaku Tsutsui,[1] Shinji Kihara,[2] Tohru Funahashi,[2] Iichiro Shimomura,[2] Shinji Tamura,[3] Shinichi Kiso[1] and Norio Hayashi[1]

Departments of [1]Gastroenterology and Hepatology and [2]Metabolic Medicine, Osaka University Graduate School of Medicine, Suita, and [3]Minoh Municipal Hospital, Minoh, Osaka, Japan

Aim: We reported previously that hypoadiponectinemia enhances hepatic oxidative stress and accelerates progression of nonalcoholic steatohepatitis (NASH) in mice. However, the precise mechanism and preventive effects of adiponectin on NASH remain unclear. The aim of this study was to examine the effects of adiponectin on steatohepatitis using adiponectin-knockout (KO) mice and adenovirus-mediated adiponectin expression system.

Methods: We used male KO mice and C57BL6/J (WT) mice fed methionine choline-deficient (MCD)-diet as a steatohepatitis model. Liver histology, hepatic oxidative stress markers, and hepatic gene expression levels were investigated. In addition, Hepa 1–6 cells, a mouse liver cell line, were cultured with or without recombinant adiponectin, and gene expressions were investigated by real-time RT-PCR.

Results: After 2-week feeding of MCD diet, hepatic steatosis was enhanced and plasma alanine aminotransferase elevated in KO mice than in WT mice. In KO mice liver, thiobarbituric acid reactive substances increased, glutathione levels decreased, and mRNA expression levels of antioxidant enzymes (catalase, superoxide dismutase-1) downregulated. Adenovirus-mediated adiponectin expression prevented these changes in KO mice. Moreover, Kupffer cell infiltration was enhanced and mRNA levels of anti-inflammatory M2 macrophage markers (interleukin-10, arginase-1) were decreased in KO mice liver. In the *in vitro* study, adiponectin significantly increased catalase gene expression in Hepa 1–6 cells.

Conclusions: Lack of adiponectin enhanced, and adiponectin administration prevented steatohepatitis progression in mice. These changes were due to the anti-oxidative effects of adiponectin, and its effects on Kupffer cells recruitment and phenotype polarization. Augmentation of adiponectin effects could be a useful preventive approach for NASH progression.

Key words: adiponectin, catalase, Kupffer cell phenotype polarization, nonalcoholic steatohepatitis (NASH), oxidative stress, PPARα

INTRODUCTION

NONALCOHOLIC STEATOHEPATITIS (NASH) is a growing medical problem in industrialized countries closely associated with obesity, insulin resistance, type 2 diabetes,[1] and considered as the hepatic phenotype of the metabolic syndrome.[2] Patients with NASH who progress to liver cirrhosis are at increased risk of hepatocellular carcinoma (HCC). Recently, obesity was recognized as an independent risk factor for NASH progression, as well as other liver diseases such as liver fibrosis,[3] chronic hepatitis C,[4,5] alcoholic liver disease,[6] and HCC.[7] However, the molecular mechanism underlying the link between obesity and NASH progression remains unknown.

The adipose tissue is an energy-storing organ that produces and secrets several bioactive substances[8,9] known as adipocytokines,[10] such as adiponectin,[11] leptin,[12] plasminogen activator inhibitor-1 (PAI-1),[10,13] and tumor necrosis factor-α (TNF-α).[14] Recent studies have suggested that obesity is a state of chronic, low-grade

Correspondence: Dr Shinichi Kiso, Department of Gastroenterology and Hepatology, Osaka University, Graduate School of Medicine, 2-2, K1, Yamadaoka, Suita, Osaka 565-0871, Japan. Email: kiso@gh.med.osaka-u.ac.jp
Received 25 November 2008; revised 20 January 2009; accepted 22 January 2009.

inflammation that contributes to insulin resistance and type 2 diabetes,[15,16] and affects not only macrophage recruitment to adipose tissue but also macrophage phenotype (pro-inflammatory macrophage (M1) and anti-inflammatory macrophage (M2)) within adipose tissue. Such inflammatory state in adipose tissue induces adipocytokine dysregulation; a decrease in insulin-sensitizing and anti-inflammatory adipocytokines such as adiponectin, and an increase in pro-inflammatory adipocytokines involved in insulin resistance such as TNF-α, interleukins, and resistin.[15–18] Recently, several studies have reported that adipocytokine dysregulation affects the pathological state of liver diseases.[19–22] For example, serum leptin and TNF-α levels were significantly higher, and adiponectin levels were significantly lower in patients with NASH than in control subjects.[20,22]

Adiponectin, a key molecule in obesity-related metabolic syndrome, has currently attracted much attention in the pathophysiology of metabolic syndrome because of its insulin-sensitizing function, anti-inflammatory properties, and anti-atherogenic function. Previously, we reported the insulin-sensitizing,[23] anti-inflammatory,[24] anti-fibrogenic[25] properties of adiponectin, and we demonstrated that the lack of adiponectin accelerated the progression of steatohepatitis in mice NASH model through enhanced oxidative stress with elevated pro-inflammatory cytokine, TNF-α, in mice serum.[26] Moreover, in a study of 80 NASH patients, hypoadiponectinemia was independently associated with NASH and with severe hepatic steatosis and necroinflammation.[22] These features suggest that adiponectin could be useful in the prevention of NASH progression. However, the precise mechanisms and preventive effects of adiponectin on steatohepatitis progression remain unclear.

The aim of the present study was to determine the role of adiponectin in the development of steatohepatitis. For this purpose, we examined the effects of methionine choline-deficient (MCD) diet on the livers of mice using adiponectin-knockout (KO) mice and an adenovirus-mediated adiponectin expression system.

METHODS

Reagents

F4/80 ANTIBODY WAS purchased from Serotec (cat. No. MCA497R; Oxford, UK). Recombinant mouse full-length adiponectin was purchased from R&D Systems (Minneapolis, MN, USA). Tyloxapol, Dulbecco's modified Eagle medium (DMEM), and fetal bovine serum were purchased from Sigma Chemical (St Louis, MO, USA).

Animal experiments

All experimental protocols and animal maintenance procedures used in this study were approved by the Ethics Review Committee for Animal Experimentation of Osaka University School of Medicine. The generation of KO mice has been described previously.[23] C57BL/6 J (WT) mice were purchased from Clea Japan (Tokyo, Japan). The animals were provided with unrestricted amounts of chow and water, housed in temperature- and humidity-controlled rooms, and maintained on a 12/12 h light/dark cycle. The MCD diet was purchased from Oriental Yeast (Osaka, Japan). This diet composition is available on request.

To investigate the effects of physiological concentrations of adiponectin on hepatic steatohepatitis, male KO ($n = 7$) mice and WT ($n = 7$) mice were fed MCD diet for 2 weeks. Control KO ($n = 7$) mice and control WT ($n = 7$) mice were fed normal chow (body weight: 23–31 g, age: 8–10 weeks). To investigate the effects of high concentrations of adiponectin on steatohepatitis, male KO mice ($n = 14$, body weight: 25–29 g, age: 10 weeks) were used. Adenovirus encoding the full-length mouse adiponectin (AdAN) and adenovirus that produces adenovirus-β-galactosidase (AdLacZ) were prepared as described previously.[23] Mice were divided into two groups (7 mice per group) and 5.0×10^6 plaque-forming units (pfu) of AdAN or AdLacZ was injected into the mice tail vein, and MCD diet was administered for 2 weeks.

In each experiment, before MCD diet administration, blood samples were collected from the tail vein after 5 h of food withdrawal, centrifuged ($13\,000 \times g$, 5 min, 4°C) and plasma was collected. At the end of the experimental period, food was withdrawn for a minimum of 5 h and then the mice were sacrificed. Blood was collected aseptically from the inferior vena cava and centrifuged ($13\,000 \times g$, 5 min, 4°C) and plasma was collected. The liver was harvested and either fixed with 10% buffered formaldehyde for histological examination, or immediately frozen in liquid nitrogen for mRNA extraction and lipid analysis.

Quantitative reverse transcription-polymerase chain reaction (RT-PCR)

Total RNA was extracted from whole liver with the QIAshredder and the RNeasy Mini kit according to the

instructions provided by the manufacturer (Qiagen, Hilden, Germany) and transcribed into complementary DNA with Quantitect Reverse Transcription kit (Qiagen). Quantitative real-time PCR was performed with QuantiFast SYBR Green PCR kit with specific primers (Qiagen) on a LightCycler according to the instructions provided by the manufacturer (Roche Diagnostics, Indianapolis, IN, USA). The primers used were PPARα (Qiagen cat. No, QT00137984), catalase (QT01058106), SOD-1 (QT00165039), CPT-I (QT00106820), MCP-1 (QT00167832), IL-10 (QT00106169), arginase-1 (QT00134288), GAPDH (QT00199388) (Qiagen). The mRNA expression levels were normalized relative to GAPDH mRNA expression level and expressed in arbitrary units.

Analysis procedures

Plasma alanine aminotransferase (ALT) concentrations were measured using the transaminase CII-test Wako kit (Wako Pure Chemical Industries, Tokyo, Japan), plasma triglycerides (TG) concentrations were measured using the TG E-test (Wako Pure Chemical Industries), plasma FFAs concentrations were measured using the NESCAUTO NEFA Kit-U (Alfresa-pharma, Osaka, Japan), plasma glucose concentrations were measured using the glucose CII-test Wako kit (Wako Pure Chemical Industries), and plasma insulin concentrations were measured using the insulin ELISA kit (Morinaga Institute of Biological Science, Yokohama, Japan). The Quantitative Insulin Sensitivity Check Index (QUICKI) was calculated for determination of insulin sensitivity[27] using fasting insulin (Ins0) and glucose (Gluc0) concentrations according to the formula 1/log (Gluc0 × Ins0).

Hepatic triglyceride contents

Total lipids were extracted from the liver as described previously.[28] Hepatic TG concentrations were determined by the colorimetric assay using the TG E-test (Wako Pure Chemical Industries).

Picro-sirius red staining

Liver sections were stained with picro-sirius red (Sigma-Aldrich). The picro-sirius red-stained area of fibrosis was quantified using image-analysis software in three randomly selected fields/section (100 × magnification). The degree of fibrosis was expressed as the percentage of the total area measured.[25]

Measurement of lipid peroxidation levels and hepatic glutathione concentrations

Liver tissue samples were homogenized in a buffer solution containing 50 mM Tris-HCl (pH 7.4) and 1.15% KCl, and then centrifuged (3000 × *g*, 10 min, 4°C). Lipid peroxidation levels in tissue-homogenate supernatants were determined as thiobarbituric acid reactive substance (TBARS) using the LPO-test (Wako Pure Chemical Industries). Liver glutathione concentrations were measured by the colorimetric assay using BIOXYTECH GSH-400 (OxisResearch, Portland, OR, USA).

Immunohistochemistry for macrophages

Tissue sections were subjected to immunohistochemical staining using a monoclonal antibody against rat anti-mouse F4/80 (1:1000). The numbers of F4/80-positive cells were counted in three randomly selected fields/section (100 × magnification).

Evaluation of hepatic very low-density lipoprotein (VLDL) secretion

KO mice ($n = 3$) and WT mice ($n = 3$) were fasted for 6 h and then injected from tail vein with 500 mg/kg of tyloxapol®, a lipoprotein lipase (LPL) inhibitor. Plasma samples were taken prior to and 30, 60, 90 min after injection, and plasma TG levels were measured.

In vitro studies

In the present study, we used a mouse liver cell line, Hepa 1–6 cell (ATCC No. CRL-1830 ™), which was obtained from American Type Culture Collection (Rockville, MD). Cells were cultured at 37°C using 5% CO_2 in the DMEM-supplemented with 10% fetal bovine serum in standard 24-well plates until 80–90% confluence and cultured in a medium containing 10% fetal bovine serum in the presence of 10 μg/mL recombinant adiponectin or vehicle for 24 h. Then, total RNA were extracted as above for measurement of mRNA expression levels of catalase, SOD-1, PPARα, and CPT-I.

Statistical analysis

The results are presented as mean ± SD. Differences between groups were examined for statistical significance using analysis of variance (ANOVA) with Fisher's PLSD test. Statistical significance was defined as $P < 0.05$.

Table 1 Biochemical analysis of plasma and liver extracts of wild-type (WT) and knock-out (KO) mice fed MCD diet for 2 weeks

	Baseline		After 2 weeks	
	WT	KO	WT	KO
Body weight (g)	30.21 ± 6.82	26.40 ± 5.89	20.83 ± 1.56	19.57 ± 5.18
Liver weight (g)	1.13 ± 0.38	1.05 ± 0.19	0.58 ± 0.06	0.50 ± 0.04
Plasma				
ALT (IU/L)	27.3 ± 11.7	23.7 ± 6.4	41.5 ± 20.7	84.6 ± 35.9
Triglyceride (mg/dL)	68.1 ± 29.8	52.6 ± 4.6	37.2 ± 8.8	36.2 ± 9.0
Glucose (mg/dL)	173.2 ± 58.2	160.2 ± 32.9	89.9 ± 9.2	97.2 ± 27.9
Insulin (pg/mL)	305.1 ± 67.37	254.51 ± 39.46	207.55 ± 57.58	280.29 ± 39.7*
QUICKI	0.213 ± 0.008	0.218 ± 0.003	0.235 ± 0.007	0.227 ± 0.009**
Liver				
Triglyceride (mg/g protein)	35.1 ± 13.5	33.5 ± 14.5	59.0 ± 15.8	84.7 ± 26.6***

*$P < 0.05$, compared with WT fed MCD diet for 2 weeks. **$P < 0.05$, compared with WT fed MCD diet for 2 weeks. ***$P < 0.05$, compared with WT fed MCD diet for 2 weeks.
ALT, alanine aminotransferase; QUICKI, Quantitative Insulin Sensitivity Check Index.

RESULTS

Animal experiments

Biochemical markers

PLASMA ALT CONCENTRATIONS increased in both KO and WT mice and tended to be higher in KO mice than in WT mice after 2-week feeding of MCD diet, compared with WT mice at baseline (0 week) (Table 1, Fig. 1a). After 2-week MCD diet, plasma TG concentrations were lower in both KO and WT mice, though statistically not different from the respective baseline values (Table 1). Furthermore, there was no difference in basal plasma insulin concentrations between WT and KO mice, but after 2-week MCD diet, the concentrations were significantly higher in KO mice than in WT mice. QUIKI values at baseline were not different between WT and KO mice, but were significantly lower in KO mice than in WT mice fed MCD diet for 2 weeks (Table 1).

Hepatic steatosis and fibrosis in mice

To investigate the direct effects of adiponectin on hepatic steatosis and fibrosis, KO and WT mice were fed MCD diet for 2 weeks. KO mice developed more severe hepatic steatosis than WT mice (Fig. 1b). Hepatic TG contents following the MCD diet were higher in KO mice than WT mice ($P < 0.01$, Table 1, Fig. 1c). In addition to hepatic steatosis, infiltration of inflammatory cells was evident in KO mice livers, whereas only a few such cells were observed in WT mice livers (Fig. 1b).

Picro-sirius red staining revealed enhanced liver fibrosis in KO mice livers, while hepatic fibrosis was scarcely seen in WT mice livers (Fig. 1d). Quantitative analysis of fibrosis showed a significantly larger fibrotic area in KO than in WT mice fed MCD diet ($P < 0.01$, Fig. 1e).

Hepatic oxidative stress in mice

To determine whether oxidative stress was enhanced in KO mice, we measured lipid peroxidation as a marker of oxidative injury. Lipid peroxidation, as reflected by hepatic TBARS concentrations, was significantly increased in KO mice compared with WT mice ($P < 0.001$, Fig. 1f). We also measured another marker of oxidative injury, hepatic glutathione (GSH), which is consumed by peroxides and reactive oxygen species. The GSH concentrations in KO mice fed MCD diet were significantly lower than their WT counterparts ($P < 0.001$, Fig. 1g). These results suggest enhanced oxidative stress in the livers of MCD diet-fed KO mice.

Hepatic gene expressions of antioxidant enzymes

To investigate the hepatic gene expressions of antioxidant enzymes in MCD diet-fed mice, we measured gene expressions of catalase and SOD-1 in the liver. The hepatic gene expression levels of both enzymes were significantly lower in MCD diet-fed KO mice than their WT counterparts ($P < 0.0001$ for catalase, Fig. 2a; $P < 0.001$ for SOD-1, Fig. 2b). There were no such differences in catalase and SOD-1 mRNA expression levels between KO and WT mice livers at baseline (Fig. 2a,b). The mRNA expression levels of hepatic PPARα, a protein upstream of catalase and SOD-1, and hepatic CPT-I, another target enzyme of PPARα, were significantly lower in MCD-fed KO mice than the respective WT mice ($P < 0.0001$ for PPARα, Fig. 2c; $P < 0.0001$ for CPT-I,

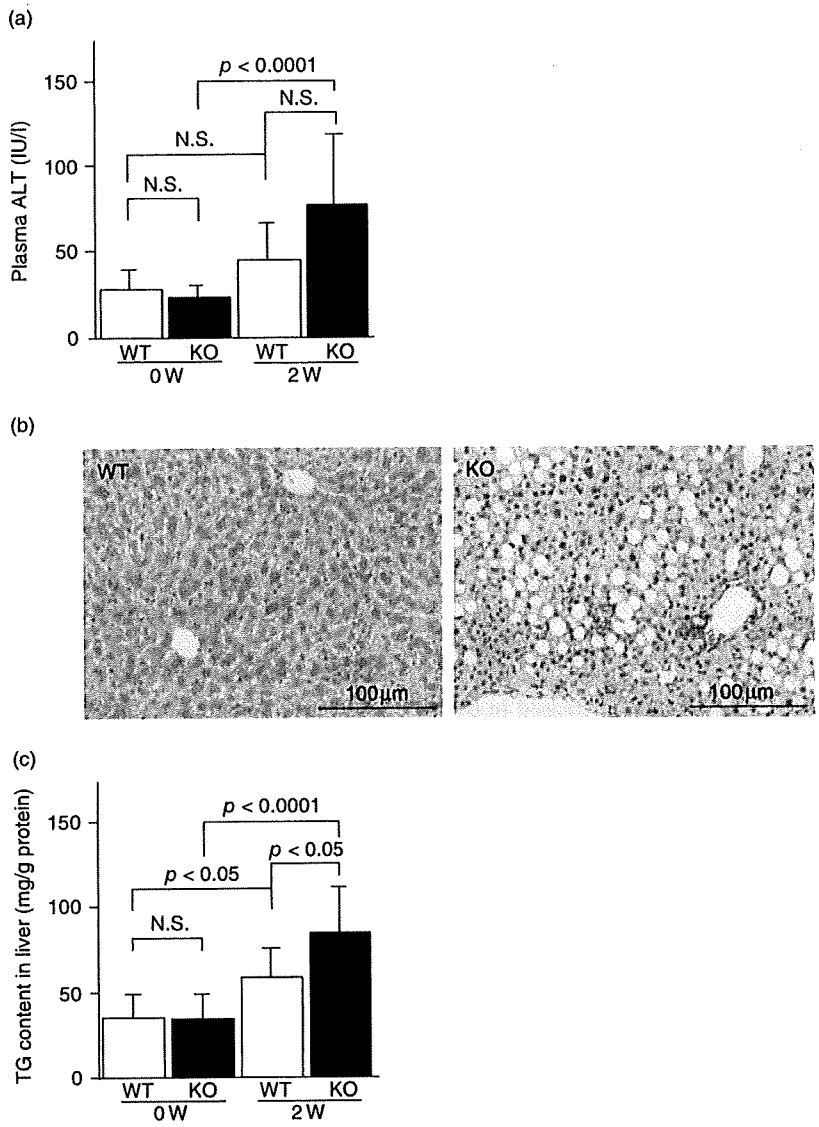

Figure 1 Liver histology, biochemical markers, and oxidative stress markers in a mouse steatohepatitis model. We used male adiponectin knockout (KO) mice and wild-type (WT) mice fed methionine choline-deficient (MCD) diet for 2 weeks as a steatohepatitis model. (a) Plasma alanine aminotransferase (ALT) concentrations before and 2 weeks after MCD diet administration. (b) Hematoxylin and eosin (H&E)-stained sections of mice livers fed MCD diet for 2 weeks. Liver sections were obtained and stained with H&E for evaluation of steatosis and inflammation. Original magnification ×200. (c) Triglyceride contents of mice livers before and 2 weeks after MCD diet administration. Total lipids were extracted from liver as described in Methods section. Hepatic concentrations of triglycerides (TG) were determined by colorimetric assay. (d) Picro-sirius red staining of mice livers fed MCD diet for 2 weeks for evaluation of liver fibrosis. Black arrows point at collagen fibers stained with picro-sirius red. Original magnification ×100. (e) Graphic representation of liver fibrosis. The fibrotic area was measured as described in the Methods section. (f) Hepatic thiobarbituric acid reactive substance concentrations were measured for evaluation of hepatic lipid peroxidation. (g) Hepatic glutathione concentrations were measured for evaluation of oxidative stress in mice. For all panels, data are mean ± SD and the *P*-values represent the results of analysis of variance with the Fisher's PLSD test.

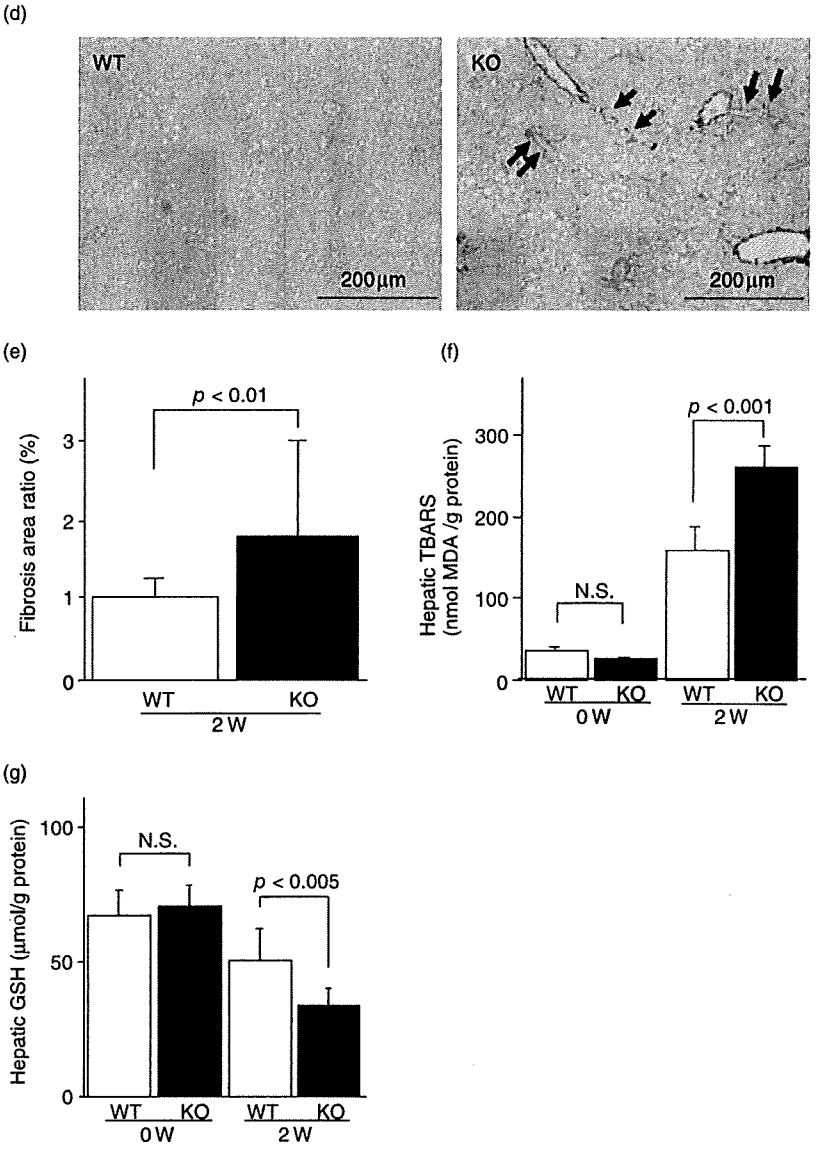

Figure 1 *Continued.*

Fig. 2d). There were no differences in mRNA expression levels of hepatic PPARα and CPT-I between the two groups of mice at baseline (Fig. 2c,d).

Hepatic gene expression of ACC in mice

To investigate the hepatic gene expression of lipogenic enzyme in mice fed MCD diet for 2 weeks, we measured the mRNA expression levels of ACC, the rate-limiting enzyme in fatty acid biosynthesis, in the liver. Hepatic ACC mRNA expression levels were significantly elevated in both MCD diet-fed WT and KO mice compared with the respective values at baseline ($P < 0.005$, Fig. 2e). However, there was no difference in mRNA expression levels between KO and WT mice at both baseline and after 2-week feeding of MCD diet (Fig. 2e).

Evaluation of hepatic VLDL secretion

To rule out possible differences in VLDL secretion from livers of KO and WT mice, we measured the rate of VLDL secretion. The response to injection of tyloxapol, an

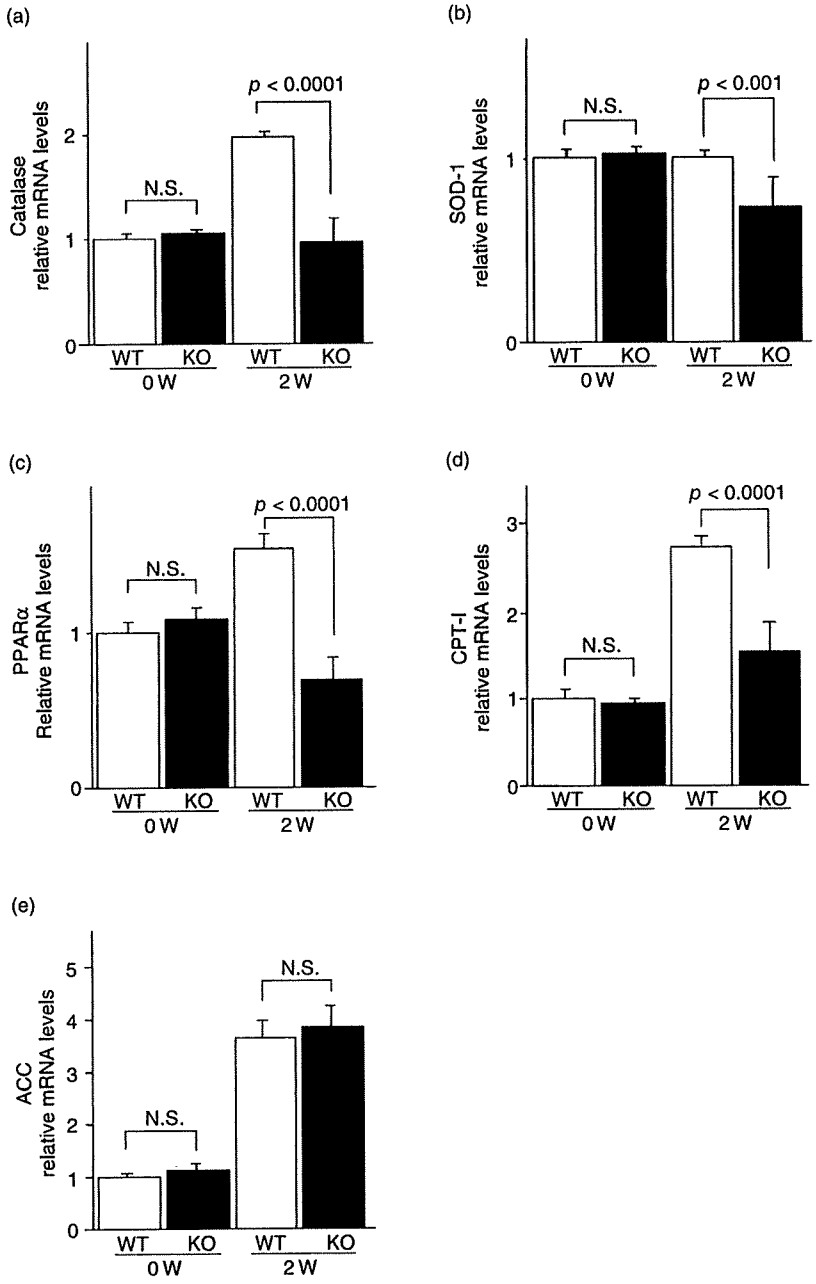

Figure 2 Gene expression levels in mice fed methionine choline-deficient (MCD) diet for 2 weeks. To investigate the hepatic gene expressions of antioxidant enzymes in knock-out (KO) mice fed MCD diet for 2 weeks, we measured the hepatic mRNA expression levels of (a) catalase and (b) SOD-1 in mice liver. We also measured hepatic mRNA expression levels of (c) PPARα, upstream of catalase and SOD-1, and (d) CPT-I, another target gene of PPARα. The gene expression of (e) ACC, a rate-limiting enzyme in fatty acid biosynthesis, was measured. The mRNA expression levels were normalized relative to the level of GAPDH mRNA expression and expressed in arbitrary units. For all panels, data are mean ± SD, and the *P*-values represent the results of analysis of variance with the Fisher's PLSD test.

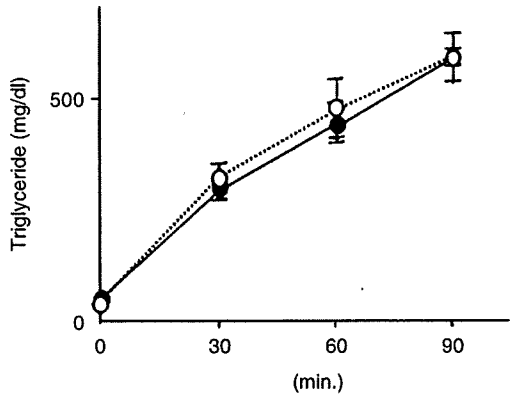

Figure 3 Evaluation of hepatic very low-density lipoprotein (VLDL) secretion from the liver. For VLDL secretion assay, knock-out (KO) and wild-type (WT) mice were injected with a single dose of tyloxapol (500 mg/kg) through tail vein. Tail blood was sampled at 30, 60, and 90 min after injection and assayed for triglycerides (TG) concentrations. Open circles: WT mice, closed circles: KO mice. Data are mean ± SD.

inhibitor of plasma lipoprotein lipases, on plasma TG concentrations measured at 30, 60 and 90 min, was not different between the two groups of mice, indicating similar hepatic VLDL secretion (Fig. 3).

Kupffer cell infiltration in mice livers

Immunohistochemical analysis of MCD-fed mice indicated significantly larger numbers of infiltrated F4/80-positive Kupffer cells (hepatic macrophage) in KO mice liver than WT mice liver (Fig. 4a,b).

M2 macrophage marker gene expressions in mice liver

To investigate the phenotype of infiltrating Kupffer cells in mice livers, we measured the hepatic mRNA expression levels of anti-inflammatory M2 macrophage markers (arginase-1 and IL-10) and MCP-1. There was no difference in hepatic mRNA expression level of arginase-1 at baseline between the two groups. After 2-week feeding of MCD diet, the hepatic arginase-1 mRNA expression level was significantly higher in WT mice than KO mice (Fig. 4c). A similar pattern was seen with IL-10, at both baseline and after MCD diet feeding (Fig. 4d). On the other hand, the hepatic mRNA expression levels of MCP-1 were higher in both KO and WT mice, compared with the baseline, and tended to be higher in KO mice than in WT mice after MCD diet feeding ($P = 0.1312$, Fig. 4e).

Effects of adenovirus-mediated adiponectin expression on mice liver

To investigate the effects of high concentrations of adiponectin on steatohepatitis progression, KO mice were injected with adenovirus producing mouse full-length adiponectin (AdAN) or adenovirus producing β-galactosidase (AdLacZ) just before MCD diet administration. Infusion of AdAN resulted in amelioration of hepatic steatosis in KO mice (Fig. 5a). Hepatic TG contents were significantly lower in AdAN-KO mice than in AdLacZ-KO mice fed MCD diet for 2 weeks ($P < 0.005$, Fig. 5b). Plasma ALT levels were significantly lower in AdAN-KO mice livers than AdLacZ-KO mice livers after 2-week feeding of MCD diet ($P < 0.0005$, Fig. 5c). Moreover, administration of AdAN suppressed the fibrotic change in KO mice livers (Fig. 5d); the area of fibrosis was significantly larger in AdLacZ-KO mice than AdAN-KO mice after 2-week feeding of MCD diet ($P < 0.01$, Fig. 5e).

Effects of AdAN administration on hepatic oxidative stress in KO mice

Hepatic TBARS concentrations were significantly lower in AdAN-KO mice than AdLacZ-KO mice ($P < 0.0001$, Fig. 5f). The GSH concentrations in AdAN-KO mice fed MCD diet were significantly higher than AdLacZ-KO mice ($P < 0.001$, Fig. 5g). These results suggest that adiponectin prevents any rise in oxidative stress in livers of MCD diet-fed mice.

Effects of AdAN administration on antioxidant enzymes gene expression levels in KO mice

Hepatic catalase mRNA expression level was significantly higher in AdAN-KO mice than AdLacZ-KO mice fed MCD diet for 2 weeks ($P < 0.001$, Fig. 6a). However, no such difference was found in hepatic SOD-1 mRNA expression (Fig. 6b). After 2 week feeding of MCD diet, the mRNA expression levels of PPARα ($P < 0.0005$, Fig. 6c) and CPT-I ($P < 0.005$, Fig. 6d) were significantly higher in AdAN-KO mice than AdLacZ-KO mice.

In vitro experiments

Effects of recombinant adiponectin on gene expression levels of antioxidant enzymes in Hepa 1–6 cells

The mRNA expression levels of catalase, PPARα and CPT-I were significantly higher in adiponectin-treated Hepa 1–6 cells than in non-treated cells ($P < 0.001$ for catalase, Fig. 7a; $P < 0.001$ for PPARα, Fig. 7c;

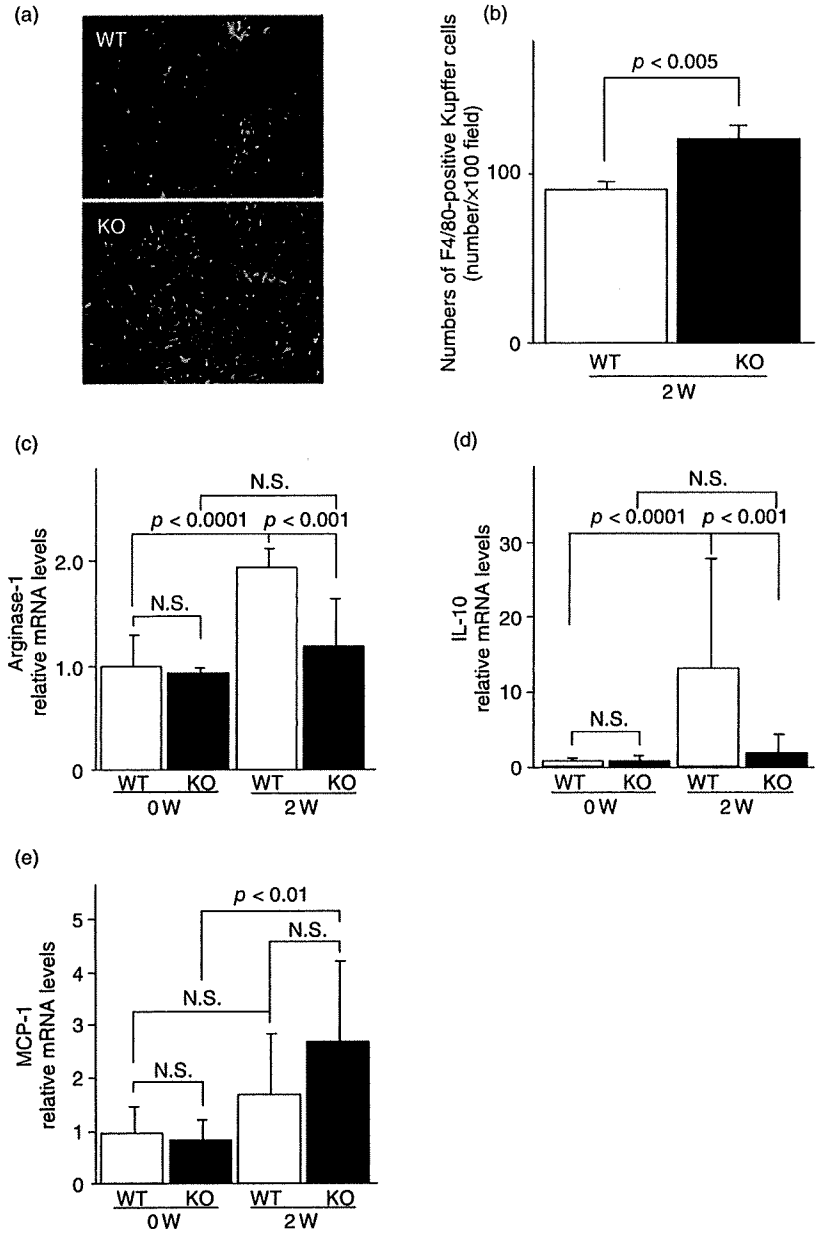

Figure 4 Hepatic Kupffer cell infiltration and gene expression levels of macrophage phenotype markers in mice livers. To investigate Kupffer cell infiltration in mice liver, liver sections were immunohistochemically stained with a rat mouodonal antibody against mouse F4/80 (1:1000). (a) The F4/80-positive Kupffer cells infiltrating the liver appeared as red spots. Original magnification ×100. (b) Graphic representation of the numbers of infiltrating F4/80-positive Kupffer cells. The numbers of F4/80 positive cells were counted in three randomly selected fields/section. (c–e), Macrophage phenotype markers gene expressions. (c) arginase-1, (d) IL-10, (e) MCP-1. The mRNA expression levels were normalized relative to the level of GAPDH mRNA expression and expressed in arbitrary units. For all panels, data are mean ± SD, and the *P*-values represent the results of analysis of variance with the Fisher's PLSD test.

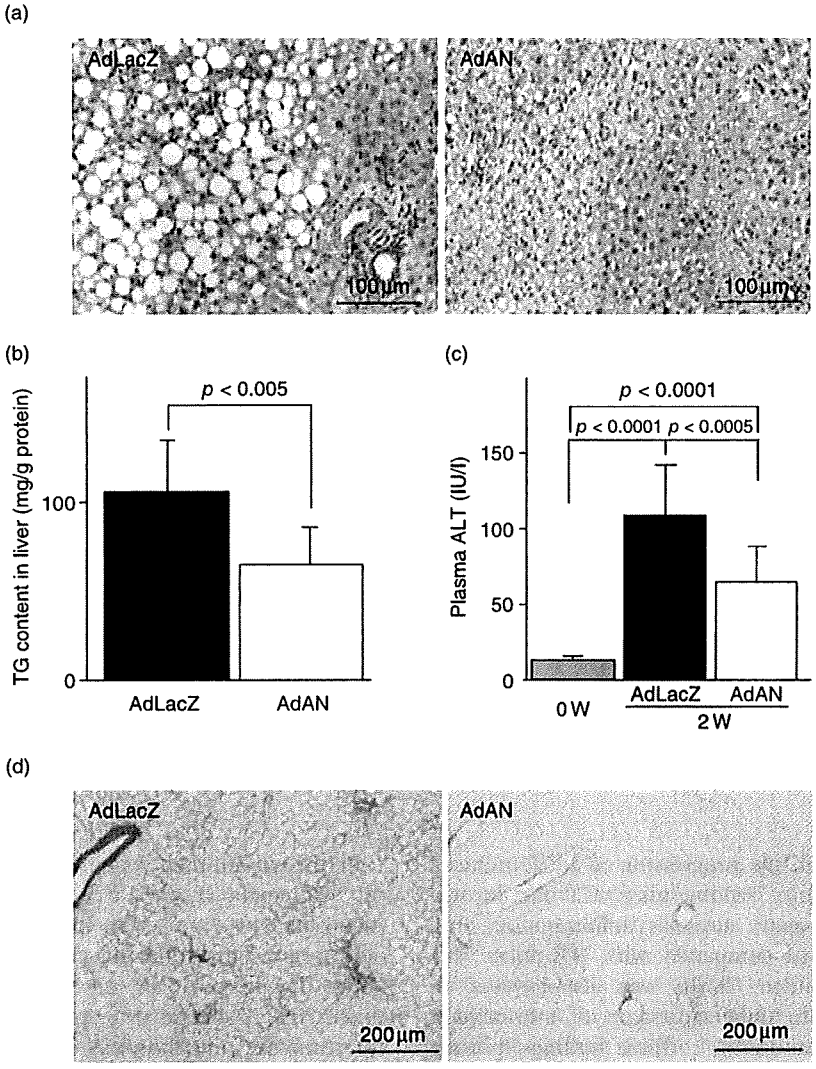

Figure 5 Effects of adiponectin administration on steatohepatitis progression in KO mice. To investigate the effects of excessive concentration of adiponectin on steatohepatitis progression, KO mice were injected with adenovirus producing mouse full-length adiponectin (AdAN) or adenovirus producing β-galactosidase (AdLacZ) just before methionine choline-deficient (MCD) diet administration. Mice were fed MCD diet for 2 weeks. (a) Hematoxylin and eosin (H&E)-stained sections of mice livers fed MCD diet for 2 weeks. Liver sections were stained with H&E for evaluation of steatosis and inflammation. Original magnification ×100. (b) Triglyceride contents of mice livers. (c) Plasma alanine aminotransferase (ALT) concentrations. (d) Picro-sirius red staining of mice livers. Original magnification ×100. (e) Graphic representation of hepatic fibrosis. (f) Hepatic thiobarbituric acid reactive substance (TBARS) concentrations measured for evaluation of hepatic lipid peroxidation. (g) Hepatic glutathione concentrations measured for evaluation of oxidative stress in mice. For all panels, data are mean ± SD, and the *P*-values represent the results of analysis of variance with the Fisher's PLSD test.

$P < 0.001$ for CPT-I, Fig. 7d). In contrast, there was no difference in SOD-1 mRNA expression level between adiponectin-treated cells and non-treated cells (Fig. 7b).

DISCUSSION

IN THE PRESENT study, we demonstrated that the lack of adiponectin accelerated, while adiponectin

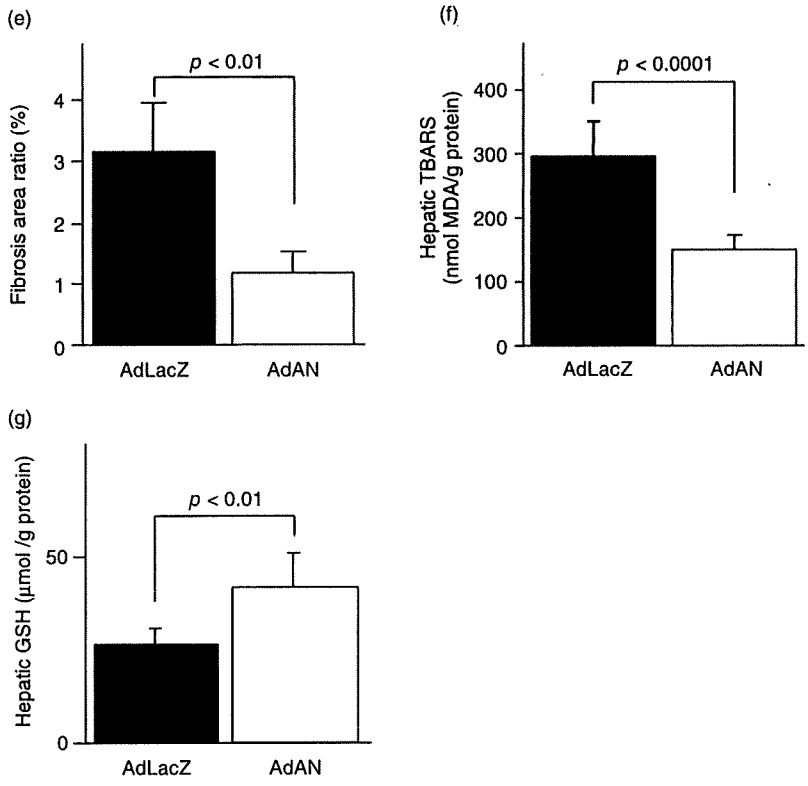

Figure 5 *Continued.*

treatment prevented the progression of MCD-induced steatohepatitis in mice. Feeding mice MCD diet for two weeks enhanced hepatic steatosis, inflammation, and fibrosis in KO mice compared with WT mice. The oxidative stress marker, TBARS, was also elevated in KO mice liver with underexpression of anti-oxidant enzymes, catalase and SOD-1. These findings indicate that at physiological concentrations, adiponectin could attenuate steatohepatitis progression through its anti-oxidant effects. In addition, we also demonstrated that supplementation of adiponectin with the injection of AdAN prevented the progression of steatohepatitis, and reversed the elevated hepatic TBARS levels and increased catalase gene expression. Moreover, in KO mice liver, the numbers of infiltrated Kupffer cells (hepatic macrophages) were increased, and MCP-1 expression was elevated compared with those in WT mice liver. However, the anti-inflammatory M2 macrophage markers, arginase-1 and IL-10, decreased in KO mice liver. These findings suggest that adiponectin can also prevent the inflammatory changes in the liver by modifying Kupffer cells phenotype polarization towards anti-inflammatory M2-Kupffer cells.

In the two-hit theory of NASH pathogenesis, the "first hit" of hepatic steatosis is followed by a "second hit", that is oxidative injury with an increase in inflammation and progression to fibrosis and HCC.[1,29] In the present study, hepatic steatosis, the first hit, developed in KO mice fed MCD diet for two weeks. Adiponectin is known to stimulate mitochondrial β-oxidation by activating PPARα and CPT-I.[30,31] In addition, we previously demonstrated that the lack of adiponectin in mice enhanced the hepatic expression of ACC, the rate-limiting enzyme in fatty acid synthesis.[26] The expression of this enzyme in MCD-fed KO mice was not elevated compared with that in the WT mice in this study, and there was no significant difference in hepatic VLDL secretion between WT mice and KO mice. These findings indicate that the lack of adiponectin enhanced hepatic steatosis through reductions in mitochondrial β-oxidation by inactivating PPARα and CPT-I in MCD diet-fed mice liver.

Oxidative stress is thought to play a crucial role in NASH progression, and adiponectin suppresses oxidative stress generation.[32] Moreover, systemic oxidative stress, as measured by urinary 8-epi-prostaglandin F2α, is strongly associated with hypoadiponectinemia.[33] We

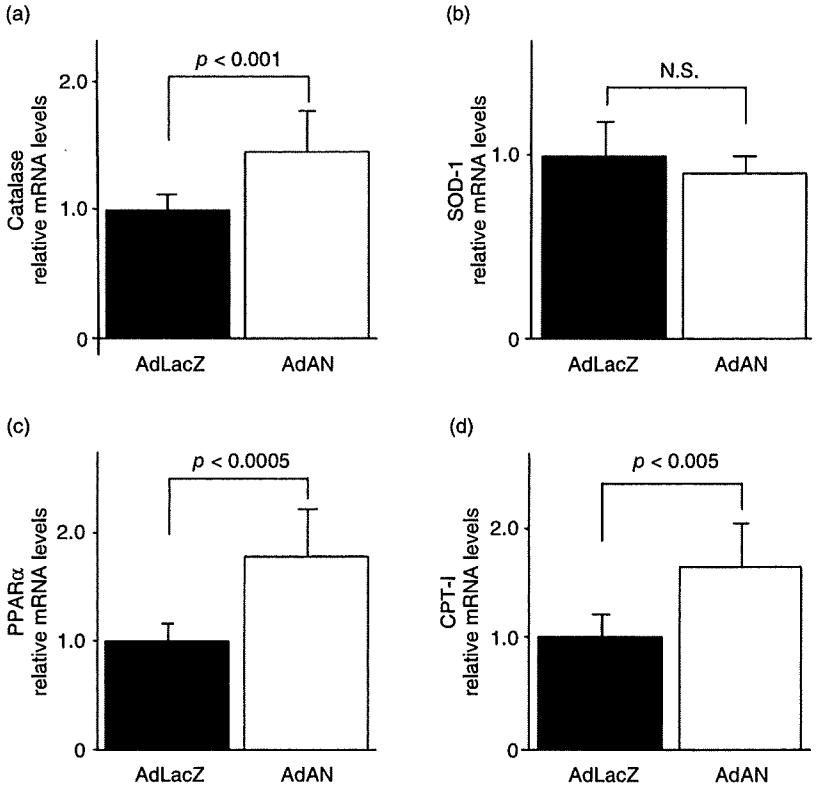

Figure 6 Effects of adiponectin administration on gene expression levels in knock-out (KO) mice. To investigate the effects of increased adiponectin levels, we measured the hepatic mRNA expression levels of (a) catalase, (b) SOD-1, (c) PPARα, and (d) CPT-I. The mRNA expression levels were normalized relative to the level of GAPDH mRNA expression and expressed in arbitrary units. For all panels, data are mean ± SD, and the *P*-values represent the results of analysis of variance with the Fisher's PLSD test.

previously reported that the lack of adiponectin accelerated the progression of steatohepatitis using another mouse NASH model [choline-deficient L-amino acid-defined (CDAA) diet (Oriental Yeast, Osaka, Japan, This diet composition is available on request.)].[25] In the CDAA diet-fed mice, the lack of adiponectin enhanced the progression of hepatic steatosis, fibrosis, and hepatic tumor formation with an increase in hepatic oxidative stress through the upregulated hepatic cytochrome P450 2E1 (Cyp2e1). In the present study, the induction of hepatic Cyp2e1 was not different between KO and WT mice livers (data not shown). This might be due to the differences in the character of MCD and CDAA diets. Our study demonstrated that the enhanced oxidative stress in KO mice liver was attributed to the downregulated anti-oxidant enzymes, catalase and SOD-1, and supplementation of adiponectin upregulated catalase expression in KO mice livers. Both catalase and SOD-1 are one of the targets of PPARα,[34] and plasma adiponectin activates hepatic PPARα through its receptor AdipoRs.[35] Our results suggest that adiponectin upregulates antioxidant enzymes through its PPARα activating effects.

Vitamin E, one of the typical antioxidant agents, has antioxidant property, and increases catalase and SOD-1 expression through the enhancement of PPARα.[36] In addition, some trials showed the effect of vitamin E treatment on NASH patient.[37,38] The effects of adiponectin on the steatohepatitis progression in this study might resemble the effects of vitamin E.

Recent studies have indicated that obesity is a chronic, low-grade inflammation state.[15,16] Moreover, additional studies demonstrated that obesity affects not only macrophage recruitment to, but also macrophage phenotype within, adipose tissue.[17,18] Macrophage phenotype has been defined across at least two separate polarization states, termed M1 (pro-inflammatory) and M2 (anti-inflammatory).[18] Macrophages are polarized toward an M2 state with IL-10 and arginase-1 expression. Hypertrophied adipocytes in obesity release chemokines, for example MCP-1, and these in turn recruit M1-polarized macrophages with low IL-10 and increased TNF-α production.[18] We reported previously that adiponectin suppresses macrophage function.[39] In addition, adiponectin suppresses TNF-α, and stimulates IL-10 production in macrophages.[26,40] We reported pre-